

1 **Assessment of PM2.5 sources and their corresponding level of**  
2 **uncertainty in a coastal urban area using EPA PMF 5.0**  
3 **enhanced diagnostics**

4 M. Manousakas<sup>(1)\*</sup>, H. Papaefthymiou<sup>(2)</sup>, E. Diapouli<sup>(1)</sup>, A. Migliori<sup>(3)</sup>,  
5 A.G. Karydas<sup>(3,4)</sup>, I. Bogdanovic-Radovic<sup>(5)</sup> and K. Eleftheriadis<sup>(1)</sup>

6 *(1) E.R.L., Institute of Nuclear & Radiological Sciences & Technology, Energy & Safety, N.C.S.R. Demokritos, 15310*  
7 *Ag. Paraskevi, Attiki, Greece*

8 *(2) Department of Chemistry, University of Patras, 26500 Patras, Achaia, Greece*

9 *(3) Physics Section, International Atomic Energy Agency, Vienna International Centre, PO Box 100, A-1400 Vienna,*  
10 *Austria*

11 *(4) Institute of Nuclear and Particle Physics, NCSR "Demokritos" 153 10 Ag. Paraskevi, Athens, Greece*

12 *(5) Ruder Boskovic Institute, Bijenicka 54, P.O. Box 180, 10002 Zagreb, Croatia*

13  
14 *\*Corresponding author: manosman@ipta.demokritos.gr*  
15  
16  
17  
18  
19  
20  
21  
22  
23

24 **Abstract**

25 Datasets that include only the PM elemental composition and no other important constituents such as  
26 ions and OC, should be treated carefully when used for source apportionment. This work is  
27 demonstrating how a source apportionment study utilizing PMF 5.0 enhanced diagnostic tools can  
28 achieve an improved solution with documented levels of uncertainty for such a dataset. The uncertainty  
29 of the solution is rarely reported in source apportionment studies or it is reported partially. Reporting  
30 the uncertainty of the solution is very important especially in the case of small datasets. PM<sub>2.5</sub> samples  
31 collected in Patras during the year 2011 were used. The concentrations of 22 elements (Z=11-33) were  
32 determined using PIXE. Source apportionment analysis revealed that PM<sub>2.5</sub> emission sources were  
33 biomass burning (11%), sea salt (8%), shipping emissions (10%), vehicle emissions (33%), mineral dust  
34 (2%) and secondary sulfates (33%) while unaccounted mass was 3%. Although Patras city center is  
35 located in a very close proximity to the city's harbor, the contribution of shipping originating emissions  
36 was never before quantified. As rotational stability is hard to be achieved when a small dataset is used  
37 the rotational stability of the solution was thoroughly evaluated. A number of constraints were applied  
38 to the solution in order to reduce rotational ambiguity.

39

40 Keywords: Source apportionment, PMF 5.0, PM<sub>2.5</sub>, PMF uncertainty

41

42

43

44

45

46

47

48

49

50

51

## 52 **Introduction**

53 Particulate air pollution has been associated with adverse effects on human health. PM is a chemically  
54 non-specific pollutant, and may originate from various emission source types. Thus, its toxicity may well  
55 vary depending on its source and chemical composition. If PM toxicity is determined with respect to  
56 source types, the regulation of PM can be implemented more effectively (Ito et al. 2006). Several factor  
57 analysis and source apportionment methods have been developed to apportion sources of ambient  
58 PM<sub>2.5</sub>. Estimates of resulting source contributions have subsequently been used in epidemiological  
59 studies to investigate the association between source-specific PM<sub>2.5</sub> and health (Kioumourtzoglou et al.  
60 2014). Given the impact of such air quality standards, it is very important to lower and assess the  
61 uncertainty of the results (Hopke et al. 2006; Kioumourtzoglou et al. 2014).

62 Greece is located at the Eastern Mediterranean basin which is characterized as air pollution hotspot,  
63 located at the crossroad of air masses coming from Asia, Europe and Africa (Karanasiou and  
64 Mihalopoulos 2013). Because of the particular characteristics of the location, PM in the area can  
65 originate from a variety of sources both local and regional. Biomass burning (Amiridis et al. 2012; Saraga  
66 et al. 2015) traffic related processes, dust resuspension (Athanasopoulou et al. 2010), industrial  
67 activities, transported Saharan dust are some of the most common sources in the area (Grigoropoulos et  
68 al. 2009; Karanasiou et al. 2009; Amato et al. 2016). In addition to those sources the climate conditions  
69 of the area (low precipitation, high solar activity) favor the accumulation of pollutants and the formation  
70 of secondary particles. For example model simulations indicate that SO<sub>2</sub> is transported in the  
71 Mediterranean basin where sulfate is produced due to intense photochemical activity (Pikridas et al.  
72 2013). The aforementioned reasons coupled with the weather conditions lead to high PM background  
73 concentrations in the area, with high impact on human health in urban areas (Ostro et al. 2014).

74 Although Greece is a coastal country with several harbors of various sizes and shipping emissions have  
75 been already identified (Karanasiou et al. 2009; Amato et al. 2016) as a source, it still remains to be  
76 adequately quantified. This source is active when the ships are in dock, as well as when they are at sea.  
77 In particular, 70% of ship emissions are estimated to occur within 400 km of the mainland (Endresen et  
78 al. 2003). Another complexity is that ships in many cases use old engine technology and that the fuel  
79 quality used is poor. Heavy oil usually contains high level of sulfur when compared with the diesel used  
80 for passenger cars and residential heating in most European countries (Fridell et al. 2008).

81 Receptor modeling using aerosol chemical composition data is a reliable method that can provide  
82 information on aerosol sources (Belis et al. 2013). Positive Matrix Factorization (PMF) (Paatero and  
83 Tappert 1994), is a receptor model that has been successfully applied to many areas with different  
84 characteristics (Querol et al. 2001; Kim et al. 2003; Johnson et al. 2006a; Moon et al. 2008; Cohen et al.  
85 2009; Amato et al. 2016; Liang et al. 2016). PMF introduces a weighting scheme taking into account  
86 errors of the data points, which are used as point-by-point weights. Adjustment of the corresponding  
87 error estimates also allows it to handle missing and below detection limit data. Moreover, non-negative  
88 constraints are implemented in order to obtain more physically meaningful factors. The latest PMF  
89 version available by USEPA, is designed to overcome some of the weak points of the previous versions of  
90 the model, providing better tools to investigate the rotational ambiguity of the factors. PMF 5.0 for the  
91 first time offers three methods for estimating uncertainty in factor analytical models: bootstrap (BS, also  
92 available on the previous versions of the model), displacement of factor elements (DISP), and bootstrap  
93 enhanced by displacement of factor elements (BS-DISP) (Paatero et al. 2014). The uncertainty of PMF  
94 analysis due to random errors and rotational ambiguity can be reduced by applying these methods.

95 In this study a small dataset was used to identify PM<sub>2.5</sub> sources in a medium-sized coastal Greek city.  
96 The elements determined in the samples by PIXE were namely Na, Mg, Al, Si, S, Cl, K, Ca, Ti, V, Cr, Mn,  
97 Fe, Ni, Cu, Zn, As, Sc, P, Ga, Co, and Ge. The concentration of all the elements except from Sc, P, Ga, Co  
98 and Ge was used as a variable in the model. This dataset was used as an example of how small datasets  
99 of PM elemental composition, could be treated and more importantly how the uncertainty of the results  
100 could be evaluated and reported. The tools offered by PMF 5.0 were used in order to evaluate the  
101 rotational stability of the solution. As rotational stability is hard to be achieved when a very small  
102 dataset is used, a number of constraints were used in the solution, so that the stability is maintained as  
103 high as possible. The application of constraints reduces the rotational space (Hopke 2016). Small dataset  
104 lead to another implication. It is hard to obtain representative source profiles without an appropriate  
105 number of samples. For example, in the manual of PMF it is suggested that for atmospheric PM at least  
106 100 samples are necessary. The application of some constraints can again improve the rotational  
107 stability and assist towards obtaining a meaningful solution.

108

## 109 **Experimental**

110

### 111 *Sampling*

112 Patras is a medium size city located in Peloponnese peninsula. Patras' population according to the last  
113 census (2011) was 168.034 citizens. It is a residential area with low industrial activity, which is mainly  
114 located in the industrial zone at the southeastern outskirts of the city. Two commercial ports are located  
115 in the area, the north or old port and the south or new port. The new port started operating at 11-Jun-  
116 2011, and it is used mainly by passenger and cargo ferries sailing to Italy. About 1.5 million passengers  
117 per year is estimated to travel using Patras' ports. Traffic in the city is high especially during rush hours.  
118 Public transport fleet is composed mainly of buses of very old technology. Olive groves are located in the  
119 surrounding area of the city. Scrap wood originating from agricultural activities is commonly used by  
120 households in close proximity to the city.



121

122 **Figure 1.** Right: Patras' location, left: sampling and potential PM2.5 sources' location

123 The sampler was installed in the city center, on the roof of a high public building (>20m) located in the  
124 central city square. The sampling site at this location allowed representative sampling of urban air from  
125 any direction. The site was selected because strong influence by nearby sources such as traffic was  
126 minimal, when compared to a kerbside station. Hence, the samples collected would be representative of  
127 the greater urban area and not be overwhelmed by the contribution of only one source. The sampler  
128 used was a low volume sampler model FRM 2000 by Rupprecht Pataschnick. This sampler is designed  
129 according to USEPA directive CFR 40. PM2.5 samples were collected onto Teflon membrane filters  
130 Whatman PTFE 47 mm diameter with 1  $\mu\text{m}$  pore size. The filter is a PTFE membrane (4 mg/cm<sup>2</sup>) with  
131 polypropylene backing. The samples were collected over a 24h sampling interval (from 00:00 to 23:59).  
132 All filters were weighed before and after sampling to determine the collected PM2.5 mass using a

133 Sartorius PB211D microbalance (readability of 0.1 µg) (Manousakas et al. 2014). Before weighing, the  
134 filters were equilibrated for 24h inside a custom designed chamber with automated controls designed to  
135 maintain environmental conditions at a constant air temperature of 20 °C and constant RH of 50%. To  
136 avoid static electricity interference the balance was equipped with a 210Po static eliminator. The filters  
137 were loaded into clean polystyrene Petri dishes and transferred to the sampling site. A number of  
138 samples were collected throughout 2011 and 55 of them were selected to be analyzed by PIXE. After the  
139 analysis the concentration of 22 elements were determined and 17 of them was used as input on the  
140 model (Na, Mg, Al, Si, S, Cl, K, Ca, Ti, V, Cr, Mn, Fe, Ni, Cu, Zn and As). The samples analyzed by PIXE were  
141 selected to equally represent the warm and cold season of the sampling period.

142 The concentration of black carbon (BC) in the collected filters was determined by optical analysis using a  
143 Smoke Reflectometer (Model 43 Smoke Stain Reflectometer, Diffusion Systems LTD). The method  
144 followed is described in detail elsewhere (Manousakas et al. 2013).

145

#### 146 *Elemental analysis, PIXE*

147 Particle Induced X-ray Emission (PIXE) was used for elemental analysis of the samples. PIXE has many  
148 advantages for elemental analysis of Particulate Matter: it provides rapid multielemental analysis  
149 capable to detect a large number of elements from Z=11 (Na) and heavier, including all the crustal and  
150 important anthropogenic elements. The advantage of a single analytical technique is the lower  
151 possibility for a random error. If a random error does occur in a PIXE measurement it is highly likely to  
152 affect all elements in a given sample, which makes it much easier to locate and treat accordingly. Of  
153 course there are drawbacks as well. It is not possible to determine all the useful PM components need in  
154 source apportionment analysis such as ions, organic carbon or some specific tracers such as  
155 levoglucosan (Kostenidou et al. 2015) and carbonate (Karanasiou et al. 2011) with a single analytical  
156 technique. The lack of those very important PM components in the analysis is very possible to lead to a  
157 solution not easily interpretable and with high levels of uncertainty. Thus, it is very important to  
158 evaluate and reduce the uncertainty.

159 PIXE measurements were performed at the Laboratory for Ion Beam Interactions, Rudjer Boskovic  
160 Institute, Zagreb Croatia. A mass calibration of the PIXE set-up has been performed utilizing Micromatter  
161 thin standards evaporated on thin Nucleopore (polycarbonate) filters. Micromatter standards are known

162 to have  $\pm 5\%$  uncertainty on areal mass concentrations (Calzolari et al. 2008). One multielemental  
163 standard (Vienna Dust Standard V98, Air particulate matter on filter media) has also been measured.  
164 PIXE set up and the calibration technique is described in detail in (Manousakas et al. 2015).

165

### 166 *Positive Matrix Factorization (PMF)*

167 The basic equation that refers to the solution of the mass balance problem is common for all the utilized  
168 multivariate receptor models including PMF:

$$169 X_{ij} = \sum_{k=1}^p g_{ik} f_{kj} + e_{ij} \quad (1)$$

170

171 Where  $X_{ij}$  is the concentration of species  $j$  measured on sample  $i$ ,  $p$  is the number of factors contributing  
172 to the samples,  $f_{kj}$  is the concentration of species  $j$  in factor profile  $k$ ,  $g_{ik}$  is the relative contribution of  
173 factor  $k$  to sample  $i$ , and  $e_{ij}$  is error of the PMF model for the  $j$  species measured on sample  $i$ . The values  
174 of  $g_{ik}$  and  $f_{kj}$  are adjusted until a minimum value of  $Q$  for a given  $p$  is found.  $Q$  is defined as:

175

$$176 Q = \sum_{j=1}^m \sum_{i=1}^n \frac{e_{ij}^2}{s_{ij}^2} \quad (2)$$

177

178 Where  $s_{ij}$  is the uncertainty of the  $j^{\text{th}}$  species concentration in sample  $i$ ,  $n$  is the number of samples, and  
179  $m$  is the number of species. In some cases other auxiliary equations can be added in order to include a  
180 priori information such as well-known chemical profiles for certain sources (Paatero and Hopke 2008;  
181 Liao et al. 2015). The auxiliary equations define the auxiliary part  $Q^a$  of object function  $Q$ :

182

$$183 Q = \sum_{v=1}^v Q_v^a = \sum_{v=1}^v \frac{r_v^2}{s_v^2} \quad (3)$$

184

185  $v$  enumerates the auxiliary equations. The residuals of auxiliary equations are denoted by  $r_v$  while  $s_v$   
186 denotes the 'softness' of  $v^{\text{th}}$  auxiliary equation, which is usually provided by the user (Paatero 1999).  
187 Those auxiliary equations can be applied to the solution in the form of constraints. Constraints can allow  
188 us identify a free rotation of the solution with better physical meaning than the original solution. In  
189 addition to that a number of rotations blocking zero values can be introduced to the matrix increasing  
190 thus the rotational stability of the solution.

191 In the current study Sc, P, Ga, Co and Ge were set as “bad” and thus were excluded from the analysis  
192 and Cr and As as “weak”. PM2.5 concentration was set as total variable.

193 A range of solutions were examined with different number of factors (4-8), but 6 factors were the  
194 maximum number of factors corresponding to meaningful sources. If the factors were increased some  
195 profiles were split creating profiles with no physical meaning, while the rotational instability of the  
196 solution increased significantly.

197 The data uncertainty was calculated by taking into account three individual errors: analytical error, PIXE  
198 calibration error and sampling error. The final uncertainty used in the model was the total uncertainty  
199 plus 1/3 LOD (Polissar et al. 1998; Lee et al. 2002; Kim and Hopke 2004; Li et al. 2004; Johnson et al.  
200 2006b). The modeling uncertainty was adjusted to 5%. Values that were much lower than LOD were  
201 substituted by ½ LOD and the uncertainty was set as 5/6 of the LOD value.

202 Small datasets (number of cases close to 50) pose an extra challenge when used for PMF because the  
203 solution is strongly affected by rotational ambiguity and the overall uncertainty is increased. Previous  
204 versions of PMF offered only “bootstrapping” as a tool to estimate the effect of random errors and to  
205 some extent the rotational ambiguity in the dataset. Fpeak was a function for estimating the lower limit  
206 of rotational uncertainty (Reff et al. 2007). The latest version gives the user more advanced tools to  
207 evaluate rotational ambiguity, namely the displacement (DISP) and the bootstrap-displacement (BS-  
208 DISP) methods. BS estimates the random errors on the matrix, while DISP explicitly explores the  
209 rotational ambiguity (Paatero et al. 2014). BS-DISP being a combination of the two methods estimates  
210 both random errors and rotational ambiguity. When the rotational ambiguity of the solution is high the  
211 identity of the resolved factors may be exchanged or swapped during DISP and BS-DISP runs. This is  
212 expressed in the diagnostic result as a number of factor swaps. In addition, the number of cases used in  
213 BS-DISP is reported, which expresses the number of accepted resamples. If all cases were accepted this  
214 number is equal to 1 (base run) plus the number of bootstraps.

215 As the base run revealed that the solution had high rotational ambiguity indicating no well-defined  
216 solutions, some physical and chemical constraints were applied in order to arrive at a more stable  
217 solution. Rotational ambiguity can be reduced among other ways by constraining individual factor  
218 elements, either scores and/or loadings, toward zero values, prescribing values for ratios of certain key  
219 factor elements (Paatero et al. 2002). It must be emphasized that application of these techniques must  
220 be based on some external information about acceptable or evidence based factor profiles. The base

221 run can be modified (constrained) by the following methods: by setting some factor elements to a fixed  
222 value, by specifying lower and/or upper limits, by pulling a factor element towards a certain value and  
223 by setting an equation such as a ratio, a mass balance equation or a custom equation. Some constraints  
224 are considered strong such as setting a variable on a fixed value because they can perturb the model  
225 results significantly. Pulling towards a value has the advantage that if the equation is incompatible with  
226 the result (Q changes too much), then the pulling will fall sort of the target value (Paatero and Hopke  
227 2008). In other words if a free rotation is not available then the pulled factor will never reach the user  
228 defined outcome. Setting constraints in the form of equations such as a ratio is regarded as a rather  
229 strong constraint but a lesser one than setting a particular value. For all other constraints apart from  
230 setting a certain value the model offers the option to set the maximum allowed dQ % change. Giving low  
231 maximum dQ% change ensures that significant perturbation of the model results are less probable.

232 After constraints were applied, BS results indicated very good reproducibility with the factors being  
233 reproduced 96-100 % of the times (88-100% before the application of the constraints). The number of  
234 bootstrap runs was set to 100 and the minimum correlation remained to the default value of 0.6. For  
235 the base run (initial unconstrained run) BS-DISP and DISP results showed 6 factor swaps for the lowest  
236 dQ change, while the cases accepted were 79%, indicating the presence of rotational ambiguity. Factor  
237 swaps are observed at the extreme case that factors change identity with no significant change in Q. The  
238 species selected to be displaced in BS-DISP, namely Na, S, Cl, K, V and PM2.5, were the key species for  
239 factor identification. It is suggested that in order to speed up computation only a small number of  
240 variables is selected for BS-DIS (Norris and Brown 2014). After the application of the constraints no  
241 factor swaps were observed for %dQ 0.5, 1 and 2 and the number of accepted cases rose to 99. The BS-  
242 DISP analysis results indicate that the solution (factor profiles) is stable. The maximum decrease in Q for  
243 the constrained run was 1%.

244 In our case not all constraints were introduced at once. The strongest were introduced first and when it  
245 was clear that the factor identity did not change, the weaker ones were applied as well. The dQ% was  
246 kept in almost all cases at the lowest value of 0.5%. The ratios applied were not significantly different  
247 from the initial run as they were not set to alter the factors but rather to keep them more rotationally  
248 stable.

249 Two of the constraints added to the analysis were in the form of elemental ratios and were derived in  
250 particular from the following equations: i) for shipping emissions:  $V - 3 \times Ni = 0$ , and ii) for biomass burning  
251  $S - 0.5 \times K = 0$ . Al, Si, Ca and Ti were pulled up maximally in the mineral dust source, BC was pulled up in

252 biomass burning and finally BC was set to zero in mineral dust. For shipping emissions V/Ni ratio the  
253 maximum allowed change in dQ was set to 5%. For all other constraints dQ was set to 0.5% making thus  
254 sure that no significant changes with respect to the unconstrained results would occur. V and Ni are well  
255 known tracers of crude oil (Viana et al. 2008, 2009; Karanasiou et al. 2009; Argyropoulos et al. 2013;  
256 Chuang et al. 2016), which is used mainly in shipping and industry. In Patras the most probable source of  
257 V and Ni is shipping, since industrial activity is low. For that reason V/Ni was set to 3 because that is the  
258 generally used ratio characteristic of shipping emissions in the Mediterranean region (Viana et al. 2009,  
259 2014). As fresh biomass burning is known to take place in Patras mainly for domestic heating and scrap  
260 wood burning from farming (Kostenidou et al. 2013; Pikridas et al. 2013), the S/K ratio in the factor was  
261 set to 0.5 which is indicative of fresh biomass burning processes (Niemi et al. 2004; Viana et al. 2013).  
262 Potassium chloride (KCl) is known to occur in fresh smoke, whereas increased amounts of potassium  
263 sulfate ( $K_2SO_4$ ) and nitrate ( $KNO_3$ ) are present in aged smoke. The S/K ratio depends on a number of  
264 factors such as the wood type and the season of the year. It must be noted that the S/K ratio in the base  
265 run had a value close to 0.5, so even though the application of this constraint comes from a rather  
266 strong assumption is considered quite safe. Another constraint that could be used was in the Na/Cl ratio  
267 for sea salt; nevertheless, the ratio obtained in the initial run was much lower than 1.8, which is that of  
268 fresh sea salt, meaning that even though the sampling station is very close to sea, extensive Cl depletion  
269 has already taken place. Trying to set such a ratio is a good example of bad use of constraints. BC was  
270 pulled up in biomass burning factor from a value of zero in the initial run, which is not considered  
271 acceptable for any combustion source profile. BC was determined using a reflectometer with analog  
272 output (Manousakas et al. 2013). Such an instrument gives an estimate of the BC concentration but it is  
273 not capable of capturing with high precision small variations in BC concentrations. This fact can lead to a  
274 more “rough around the edges” distribution of BC in the PMF factors. The presence of other key  
275 compounds for the identification of this source like OC (Organic Carbon), would have helped in getting a  
276 clearer profile. The very low dQ change allowed ensures that no big changes were imposed on the  
277 factors. The strongest constrained applied was BC set to zero in the Mineral dust factor. That was  
278 considered necessary in order to introduce to the matrix more rotation blocking zero values. Mineral  
279 dust as a source is not expected to produce any BC so setting its concentration to zero is regarded as a  
280 rather safe option. Of course the possibility that some BC is transferred along with mineral dust cannot  
281 be excluded. This constraint might add a small subjectivity to the analysis. After all the constraints were  
282 applied, the factors prior and after their application were examined and compared to investigate the

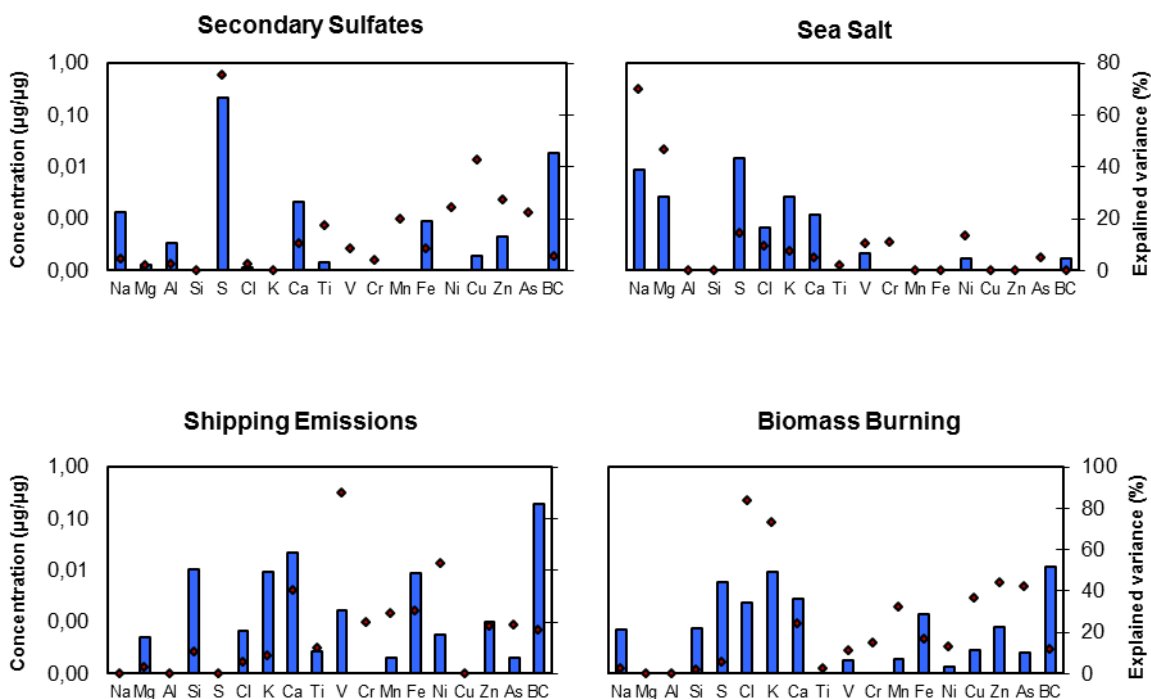
283 changes that have occurred. No significant changes to either the profiles or the contributions were  
284 observed meaning that the identity of the factors remained the same in all cases.

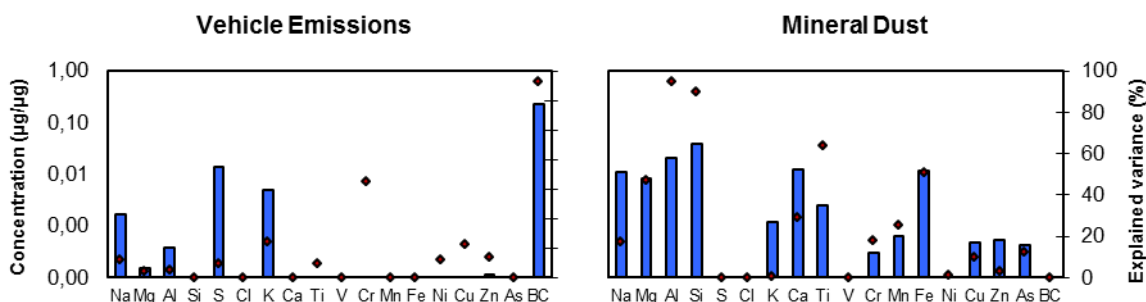
285

## 286 Results and Discussion

### 287 Source apportionment Results

288 Six factors were found to be the maximum number of physically meaningful factors for the city of  
289 Patras. This number of fine aerosol sources is identified in a number of studies conducted in other Greek  
290 Urban environments (Mantas et al. 2014; Manousakas et al. 2015). Good correlation was observed  
291 between the model predicted and the real PM<sub>2.5</sub> mass ( $R^2=0.80$ ,  $y = 1,00x - 0.30$ ). Theoretical Q and  
292  $Q_{\text{robust}}$  displayed a 25% difference. As stated before the extra modeling uncertainty was set to 5%.

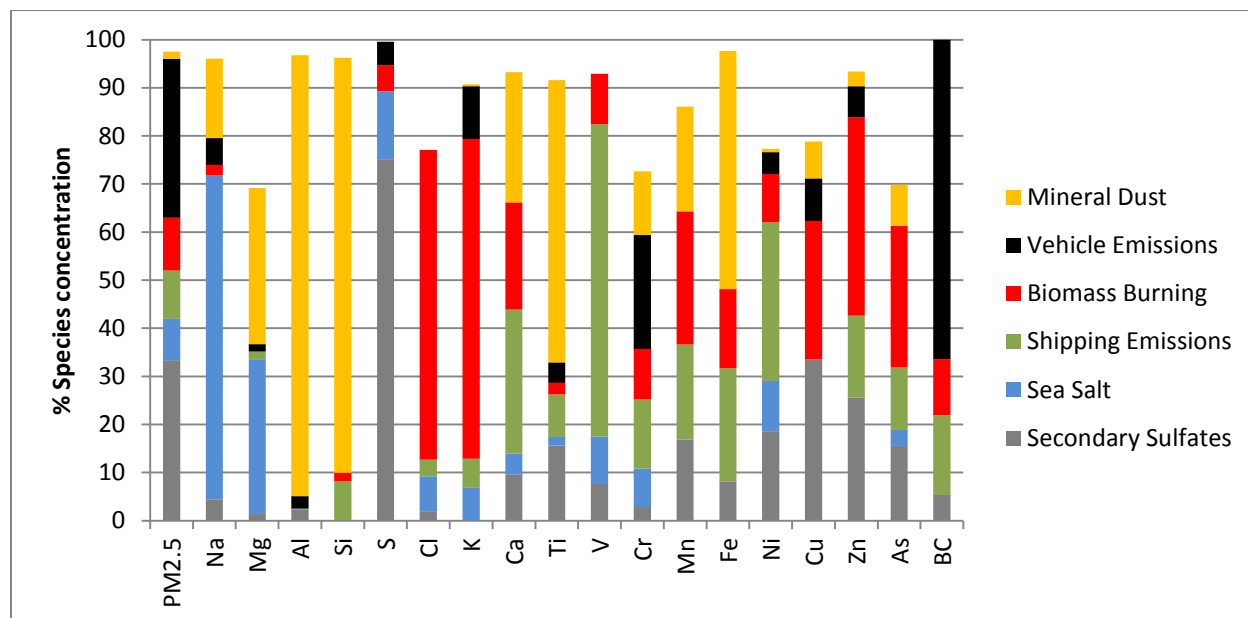




293 **Figure 2.** PMF factors profiles for the identified sources

294 The first factor (Figure 2) was identified as secondary sulfates because of the high abundance of S in the  
 295 source profile (Figure 3). The profile also contains a substantial proportion of elements related to  
 296 vehicular traffic, and in particular tire/break wear (such as Cu and Zn), indicating possible influence by  
 297 non-exhaust traffic emissions as well. Secondary inorganic aerosols are formed from the reaction of  
 298  $\text{H}_2\text{SO}_4(\text{g})$  and  $\text{HNO}_3(\text{g})$  with  $\text{NH}_3$ , giving  $(\text{NH}_4)_2\text{SO}_4$  and  $\text{NH}_4\text{NO}_3$  accordingly (Stockwell et al. 2003;  
 299 Squizzato et al. 2013). The main tracers of this source are  $\text{SO}_4^{2-}$  and  $\text{NH}_4^+$  but  $\text{NO}_3^-$  may also be present in  
 300 the source profile, when the factor represents inorganic aerosols in general rather than secondary  
 301 sulfates exclusively (Yin et al. 2005; Viana et al. 2008). Since the formation of  $(\text{NH}_4)_2\text{SO}_4$  and  $\text{NH}_4\text{NO}_3$  is  
 302 usually favored in different seasons, the concentrations of these two secondary species do not have high  
 303 correlation and they tend to be apportioned in separate factors. Because the concentration of major  
 304 ions was not available in the current dataset, S was used as the main tracer to identify this source, a  
 305 practice that has been previously applied in other studies (Marcazzan et al. 2003). The absence of the  
 306 major ions and especially  $\text{NO}_3^-$  can add some implications to the results because the mass of the  
 307 secondary nitrates can be apportioned to others sources such as traffic or biomass burning. Secondary  
 308 sulfates represent a high percentage in the mass of  $\text{PM}_{2.5}$  in Greek urban environments with regional  
 309 origin. This result is in agreement with those reported for the Greater Athens Area (Pateraki et al. 2012;  
 310 Mantas et al. 2014; Dimitriou et al. 2015). Secondary sulfates are in many cases attributed to long range  
 311 transport events (Viana et al. 2008). Previous studies have stated that sulfates are ingredients of the  
 312 “aged” air masses, because the oxidation of  $\text{SO}_2$  to  $\text{SO}_4^{2-}$  is slow (Querol et al. 1998), and thus this  
 313 aerosol component is more related to transported than local pollution (Eleftheriadis et al. 1998; Ricard  
 314 and Jaffrezo 2002; Schaap et al. 2004; Saffari et al. 2013). High sulfate concentrations due to transport  
 315 have been known to influence Greece, as documented by the high levels observed in background areas

316 in the Aegean (Gerasopoulos et al. 2006; Lazaridis et al. 2006). This source has the highest contribution  
 317 along with vehicle emissions ( $7.21 \mu\text{g}/\text{m}^3$ , accounting for 33% of total PM<sub>2.5</sub> mass on average, Figure 4).



318

319 **Figure 3.** Source fingerprints

320 The factor representing sea salt has been identified by the high contribution of Na and Mg. Sea spray is  
 321 commonly identified as a source of PM and especially PM<sub>10</sub> in southern European Countries (Viana et  
 322 al. 2008; Bove et al. 2016). Cl is present in the factor but in much lower concentration than expected for  
 323 sea salt by stoichiometry. The Cl depletion in the factor indicates that the sea salt cannot be  
 324 characterized as fresh but rather as aged. Fresh sea salt is almost exclusively found at the coarse particle  
 325 fraction (Eleftheriadis et al. 2014), and that is probably the reason why fresh sea salt is not identified as  
 326 a source despite that sampling in this study took place in very close proximity to the sea. Sea salt has a  
 327 contribution of 8% which remains very stable throughout the seasons.

328 Shipping emissions are identified by the high presence of Ni and V in the factor along with the presence  
 329 of Fe. All of them are common tracers of crude oil burning (Karanasiou et al. 2009; Argyropoulos et al.  
 330 2013). This source is common in the Mediterranean region (Waked et al. 2014; Amato et al. 2016). As  
 331 mentioned before the ratio of V/Ni was constrained to 3 for this factor (was 2.6 in the initial base run),  
 332 which is an indicative value for shipping emissions in the Mediterranean region. BC is present in the  
 333 factor as expected in all combustion processes. Since there are no refineries or oil powered plants in the  
 334 area it is safe to say that the contribution of this source can be attributed to shipping alone. The

335 contribution of this source is 10% of PM<sub>2.5</sub> on annual basis and is higher during the warm season  
336 probably because of the higher vessel related activity that peaks during that period.

337 Biomass burning is resolved mainly by the presence of high K concentrations and to a lesser extent by  
338 presence of Cl in the factor (Diapouli et al. 2014). As mentioned biomass burning in the area of Patras is  
339 related mainly to farming processes, and specifically to scrap wood burning at olive groves and  
340 agricultural fires in the region. In addition to that, due to the economic crisis and the increased prices of  
341 diesel (diesel based central heating was the most common means of domestic heating in Greece),  
342 biomass burning use for domestic heating has dramatically increased in the last years (Saffari et al.  
343 2013). K in fresh smoke is in the form of KCl which explains the high abundance of this element in the  
344 factor (Viana et al. 2013). Additionally it is quite common that plastic waste is burned in fires along with  
345 the biomass, leading to fresh particle formation with up to 21% concentration of Cl (Kostenidou et al.  
346 2013). This source has 11% contribution and is manifested almost exclusively in the cold season (Table  
347 1).

**Table 1.** Source contribution in  $\mu\text{g}/\text{m}^3$  annually and for the cold and warm season of the year

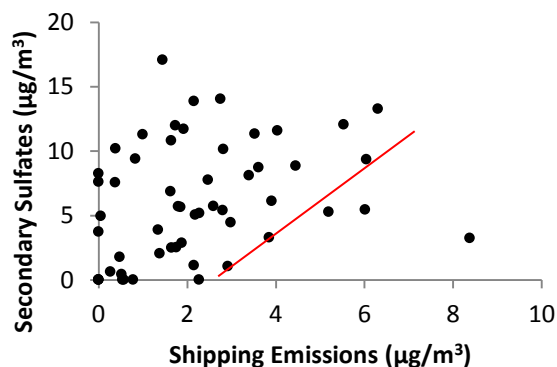
	<b>Secondary Sulfates</b>	<b>Sea Salt</b>	<b>Shipping Emissions</b>	<b>Biomass Burning</b>	<b>Vehicle Emissions</b>	<b>Mineral Dust</b>
<b>Annual</b>	7.2	1.9	2.2	2.4	7.1	0.3
<b>Warm</b>	7.5	1.7	2.9	0.8	4.5	0.3
<b>Cold</b>	7.0	1.9	1.7	3.4	8.8	0.3

348

349 Vehicle exhaust emissions are traced by the high percentage of BC in the factor and the lower presence  
350 of Cu, Zn, K, and Cr. A vehicle non-exhaust factor has not been identified, probably because of the  
351 elevated position of the sampler and the small number of samples. The elevated position of the sampler  
352 made resuspension sources less influential. In addition, non-exhaust emissions generally contribute  
353 more to coarse rather than fine particles. The chemical profile obtained for this vehicle exhaust source,  
354 consists mainly of BC. The old technology buses, which are the only means of public transport in the city,  
355 as well as the many trucks that circulate in the port area, are expected to influence this source the most.  
356 The contribution of this source is 33% and it is higher on the cold period of the year probably due to the  
357 lower inversion layer, which limits the dilution of vehicular emissions during the winter season (Khillare  
358 and Sarkar 2012).

359 Mineral dust is a well-defined factor identified by the high concentration of the crustal elements such as  
360 Al, Si, Ca, Ti and Fe. Al, Si, Ca and Ti are expected to originate mainly from this source. The contribution  
361 of this source is very small (2%) and stable throughout the year. Even though this source is not expected  
362 to have high contribution in PM<sub>2.5</sub>(Eleftheriadis and Colbeck 2001) it is expected that it is also  
363 influenced by the high sampling location.

364 Generally no correlations are expected to exist between the sources, as each source contributes aerosol  
365 to the receptor independently from others. Examination of the scatter plot of secondary sulfates and  
366 shipping emissions contributions, reveals a lower edge in the data points, indicating that for high  
367 shipping emissions the secondary sulfates are also high (Figure 5). Ships can emit SO<sub>3</sub> which is  
368 transformed very fast to sulfates (Kim and Hopke 2008; Pandolfi et al. 2011). Combustion of residual oil  
369 will also produce particles containing vanadium (V) and nickel (Ni). Vanadium reacts with the oxygen  
370 from the combustion air surplus creating V<sub>2</sub>O<sub>5</sub> that forms layers on the heat exchanger and other boiler  
371 and stack surfaces. The V<sub>2</sub>O<sub>5</sub> acts as a catalyst in the temperature range of 500–800 °C, accelerating the  
372 SO<sub>3</sub> formation. SO<sub>3</sub> formed by this mechanism can exceed the amount produced in the flame by a factor  
373 of two or three (Kim and Hopke 2008). Therefore, part of secondary sulfates may be associated with  
374 shipping emissions. The absence of S from the shipping emissions might be another indication that  
375 partially shipping emissions are recognized by the model as secondary sulfates. The lack of ions in the  
376 analysis makes it hard for factors such as secondary sulfates to be very “selective”. That means that  
377 even though this source can be identified because of its high contribution, probably S originating from  
378 other processes is also accumulated in the factor.



379

380 **Figure 5.** G space plot between secondary sulfates and shipping emissions

381

382 *Result Evaluation*

383 The constrained applied first helped “clear” the factor profile from the “noise” that is present in the  
 384 form of elements that are not related to the source itself. This problem is of course more pronounced in  
 385 the case of small datasets and especially when the constituents included in the analysis represent only a  
 386 small fraction of total PM mass. The elements of crustal origin being pulled up in the mineral factor and  
 387 BC pulled up in the biomass burning factor are examples of the first type of constraints. The second type  
 388 are constraints applied for reducing the rotational ambiguity of the factors. Rotational ambiguity is  
 389 decreased when a sufficient number of zero values in G and F matrixes are present (Paatero and Hopke  
 390 2008). Assigning fixed values to either F or G will have the same result as zero values but it might be a  
 391 more subjective choice. Known elemental ratios fixed for certain source profiles and BC pulled to zero  
 392 are examples of this type of constraints.

**Table 2.** Uncertainty tools’ results for PM2.5 mass concentration ( $\mu\text{g}/\text{m}^3$ )

	Base Value	BS 5th	BS Median	BS 95th	BS-DISP 5th	BS-DISP Average	BS-DISP 95th	DISP Min	DISP Average	DISP Max
Secondary Sulfates	7.1	4.9	7.0	7.2	0.8	5.0	9.2	5.7	6.9	8.1
Sea Salt	1.8	0.0	3.0	3.4	0.0	2.1	4.1	0.9	1.8	2.6
Shipping Emissions	2.2	2.5	2.8	3.1	1.1	3.9	6.7	1.6	2.4	3.2
Biomass Burning	2.3	0.6	0.8	0.9	0.6	5.1	9.6	2.8	3.3	3.8
Vehicle Emissions	7.1	4.2	6.9	7.4	0.4	5.0	9.6	5.6	6.5	7.4
Mineral Dust	0.3	0.0	0.5	0.8	0.0	3.4	6.9	0.1	0.6	1.1

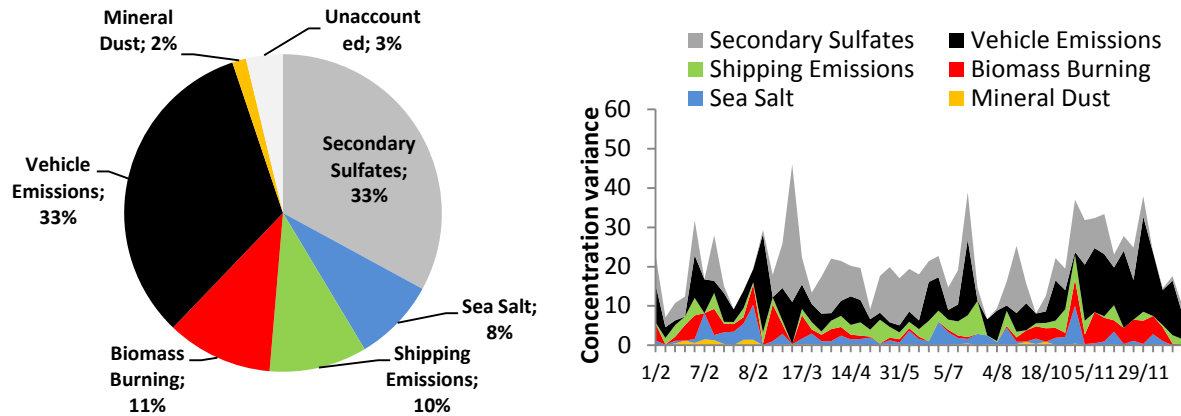
393  
 394  
 395  
 396

**Table 3.** Uncertainty tools' results for specific elements used as tracers of particular sources, where: SSU secondary sulfates, SEA sea salt, SHI shipping emissions, BIB biomass burning, VEH vehicle exhaust and MID mineral dust

	Source	Base Value	BS 5th	BS Median	BS 95th	BS-DISP 5th	BS-DISP Average	BS-DISP 95th	DISP Min	DISP Average	DISP Max
S	SSU	1.789	1.496	1.132	1.389	3.169	0.888	1.250	1.612	1.236	1.512
Na	SEA	0.200	0.141	0.162	0.234	1.084	0.104	0.145	0.186	0.130	0.165
V	SHI	0.005	0.004	0.001	0.003	0.005	0.000	0.002	0.004	0.003	0.004
K	BIB	0.271	0.217	0.025	0.068	0.103	0.148	0.210	0.273	0.217	0.244
BC	VEH	1.601	1.648	1.143	1.583	3.049	0.635	1.120	1.604	1.287	1.444
Si	MID	0.279	0.231	0.049	0.203	0.434	0.236	0.264	0.292	0.244	0.262

397

398 In Tables 2 and 3 the results from the uncertainty tools offered by PMF 5.0 are presented. The results  
399 provided in Table 2 are based on PM2.5 concentration for each source. Mineral dust has high  
400 uncertainty as expected by the low contributing mass concentration of this source. For secondary  
401 sulfates and vehicle emissions the results are quite stable as indicated by the three rotational tools. The  
402 higher uncertainty for BS and BS-DISP, indicates that a number of peak events affect these factors.  
403 Those events might not be resampled in the BS runs leading to higher uncertainty. The time series of  
404 24h source contributions presented in Figure 4, reveals that such events do exist. A matter of discussion  
405 is whether such events should be considered as outliers and be subsequently removed from the  
406 analysis. It is noted here that after the first model run the results were evaluated in order to locate any  
407 possible outliers in the dataset. After the convergence of the PMF algorithm the program calculates the  
408 residuals and identifies the points of bad fit (Paatero and Tappert 1994). For the small number of such  
409 cases identified, their corresponding uncertainties were increased thus their significance in the fitting  
410 was decreased. Events of episodic nature such as forest fires or intense long range transport events may  
411 appear as outliers, but if they are down weighted, then a serious modeling error is made, leading to loss  
412 of critical information (Paatero et al. 2014).



413

414 **Figure 4.** Source contributions and their time variability

415 Sea salt seems to have a similar uncertainty level as secondary sulfates and vehicle emissions, with BS  
 416 tests yielding the highest uncertainty. Unlike the sources discussed so far, in the case of sea salt  
 417 resampling is not assured for both low (or even zero values) and peak events instead of peak events  
 418 only, affecting the uncertainty. Shipping emissions seem to be more sensitive to BS-DISP even though BS  
 419 and DISP when tested separately produce similar results. Generally speaking sources identified only by a  
 420 small number of elements are much more sensitive to DISP based analysis. Biomass burning has the  
 421 highest uncertainty for all three tests. Biomass burning has either very high (cold season) or very  
 422 low/zero (warm season) contributions and it is identified mainly by one element (K), thus it is very  
 423 sensitive both to resampling and displacement. Generally speaking high uncertainties are to be expected  
 424 when small datasets are used (Paatero et al. 2014).

425 The uncertainties provided by the rotational tools correspond to profile uncertainties. The uncertainty  
 426 given on Table 2 regarding PM<sub>2.5</sub> applies also to estimates of average PM<sub>2.5</sub> contribution from each  
 427 factor because all modeling is performed under the constraint that average G values must be normalized  
 428 for each factor with respect to mass (Paatero et al. 2014). A straightforward method to calculate  
 429 uncertainty for individual (24-h) contribution values does not yet exist, although intercomparison  
 430 studies has given some indications towards this direction (Belis et al. 2015). An approach using  
 431 regression analysis is proposed in this work. The error of the source contribution was calculated based  
 432 on the standard error of the coefficients of a multiple regression between the daily PM<sub>2.5</sub> concentration  
 433 (independent variable) and the six source contributions for any given day (dependent variables). The  
 434 regression approach assumes that all the factors that explain the mass are identified. However, if a  
 435 significant portion of the mass that is not directly correlated with the species that are in the PMF

436 analysis is missed, the source contributions will be overestimated. This might be an important source of  
437 additional uncertainty. Results are shown in Table 4. It must be noted that this method captures only  
438 one part of the uncertainty, because it does not include the error arising from the profile uncertainty  
439 and the rotational ambiguity. Using this method we can investigate how well the daily contributions can  
440 recreate the daily PM mass. Since the correlation of the model predicted mass and the true PM mass is  
441 high ( $R^2= 0.80$ ) it is believed that this method could provide an estimate of this uncertainty.

442

**Table 4.** Sources contribution and corresponding error in  $\mu\text{g}/\text{m}^3$

	Contribution	Err
Secondary Sulfates	7.2	0.1
Sea Salt	1.9	0.6
Shipping Emissions	2.2	0.6
Biomass Burning	2.4	0.5
Vehicle Emissions	7.1	0.2
Mineral Dust	0.3	0.2

443

444 The errors calculated by this method are quite low indicating a good model fit. Mineral dust because of  
445 its very low contribution has a high error assigned to its contribution.

446 In Table 3 the uncertainty of the main elements used as tracers for each source are presented. Those  
447 results are very useful because they are needed in order to evaluate which factors may be more reliably  
448 attributed to sources, by showing which components were fitted confidently and which components  
449 were too uncertain to be considered for source identification. All elements uncertainties are considered  
450 reasonably low and thus the factors can be indeed identified as specific PM sources. The only element  
451 that shows quite high uncertainty for BS is K probably because of the variability in concentrations it has,  
452 making it very sensitive on resampling. DISP result for the same element is much more stable.

453

#### 454 *Conclusions*

455 A small dataset of 55 samples was used in order to identify the sources of PM<sub>2.5</sub> in Patras. The target of  
456 the study, apart from source identification and characterization, was to evaluate the stability of the

457 solution resulting from the use of a small dataset, using the tools offered by PMF 5.0. When no  
458 constraints are applied, the results from the base run were characterized by high uncertainty, to the  
459 extent that no sources could be attributed to the factors. After the application of the constraints the  
460 solution was stable and could be interpreted in a meaningful manner.

461 The constraints applied were in the form of elemental ratios and in particular for shipping emissions ( $V -$   
462  $3 \times Ni = 0$ ) and for biomass burning ( $S - 0.5 \times K = 0$ ). Al, Si, Ca and Ti were pulled up maximally in the mineral  
463 dust source, BC was pulled up in biomass burning and finally BC was set to zero in mineral dust. The  
464 change in Q after the application of the constraints was low (<1%).

465 Six sources were identified and were namely biomass burning (11%), shipping emissions (10%), sea salt  
466 (9%), secondary sulfates (34%), mineral dust (2%) and vehicle emissions (34%). This is the first time that  
467 the contribution of shipping emissions is quantified in a Greek urban area with port. This information  
468 can be used for the development of more effective measures for the improvement of the air quality of  
469 the area.

470 BS, DISP and BS-DISP results showed that the profile uncertainty for the elements used as tracers for  
471 factor identification was quite low, providing strong evidence for the identification of the factors. PM2.5  
472 concentration in the profiles has high uncertainty in some cases, a fact that is attributed mainly to the  
473 small dataset and the high level of uncertainty assigned to PM2.5 when set as total variable (uncertainty  
474 is tripled in that case). The case of biomass burning revealed that sources with high seasonal variability  
475 are especially vulnerable to resampling techniques in small datasets.

476 Overall the results indicate that the use of the tools offered by PMF 5.0 and the consideration of  
477 appropriate constraints significantly improve the solution even for data sets of limited number of  
478 samples. It is very important to fully report the uncertainty of the solution in source apportionment  
479 studies especially if small datasets are used. In any case it should be noted that this work does not  
480 encourage the use of small datasets, and datasets with a larger number of samples should be used  
481 whenever possible.

#### 482 *Acknowledgements*

483 This work has been supported by the European Community as an Integrating Activity 'Support of Public  
484 and Industrial Research Using Ion Beam Technology (SPIRIT)' under EC contract no. 227012. Financial

485 support from the EnTeC FP7 Capacities program (REGPOT-2012-2013-1, FP7, ID: 655 316173) and K.  
486 Karatheodori program (Grand D165) are also acknowledged.

487

488

489 *References*

490 Amato F, Alastuey A, Karanasiou A, Lucarelli F, Nava S, Calzolari G, et al. AIRUSE-LIFE + : a harmonized PM  
491 speciation and source apportionment in five southern European cities. *Atmos Chem Phys*.  
492 2016;16:3289–309.

493 Amiridis V, Zerefos C, Kazadzis S, Gerasopoulos E, Eleftheratos K, Vrekoussis M, et al. Impact of the 2009  
494 Attica wild fires on the air quality in urban Athens. *Atmos Environ* [Internet]. Elsevier Ltd;  
495 2012;46:536–44. Available from: <http://dx.doi.org/10.1016/j.atmosenv.2011.07.056>

496 Argyropoulos G, Grigoratos T, Voutsinas M, Samara C. Concentrations and source apportionment of  
497 PM10 and associated elemental and ionic species in a lignite-burning power generation area of  
498 southern Greece. *Environ Sci Pollut Res Int* [Internet]. 2013 Oct [cited 2014 Jan 30];20(10):7214–  
499 30. Available from: <http://www.ncbi.nlm.nih.gov/pubmed/23644947>

500 Athanasopoulou E, Tombrou M, Russell AG, Karanasiou A, Eleftheriadis K, Dandou A. Implementation of  
501 road and soil dust emission parameterizations in the aerosol model CAMx: Applications over the  
502 greater Athens urban area affected by natural sources. *J Geophys Res Atmos*. 2010;115(17):1–21.

503 Belis CA, Karagulian F, Larsen BR, Hopke PK. Critical review and meta-analysis of ambient particulate  
504 matter source apportionment using receptor models in Europe. *Atmos Environ* [Internet]. Elsevier  
505 Ltd; 2013 Apr [cited 2014 Jun 3];69:94–108. Available from:  
506 <http://linkinghub.elsevier.com/retrieve/pii/S1352231012010540>

507 Belis CA, Pernigotti D, Karagulian F, Pirovano G, Larsen BR, Gerboles M, et al. A new methodology to  
508 assess the performance and uncertainty of source apportionment models in intercomparison  
509 exercises. *Atmos Environ* [Internet]. Elsevier Ltd; 2015;119:35–44. Available from:  
510 <http://linkinghub.elsevier.com/retrieve/pii/S1352231015302478>

511 Bove MC, Brotto P, Calzolari G, Cassola F, Cavalli F, Fermo P, et al. PM10 source apportionment applying  
512 PMF and chemical tracer analysis to ship-borne measurements in the Western Mediterranean.  
513 *Atmos Environ*. 2016;125:140–51.

514 Calzolari G, Chiari M, Lucarelli F, Mazzei F, Nava S, Prati P, et al. PIXE and XRF analysis of particulate  
515 matter samples: an inter-laboratory comparison. *Beam Interact with Mater Atoms* [Internet]. 2008  
516 May [cited 2013 Feb 14];266(10):2401–4. Available from:  
517 <http://linkinghub.elsevier.com/retrieve/pii/S0168583X08002772>

518 Chuang M-T, Chen Y-C, Lee C-T, Cheng C-H, Tsai Y-J, Chang S-Y, et al. Apportionment of the sources of  
519 high fine particulate matter concentration events in a developing aerotropolis in Taoyuan, Taiwan.  
520 *Environ Pollut* [Internet]. Elsevier Ltd; 2016;214:273–81. Available from:  
521 <http://linkinghub.elsevier.com/retrieve/pii/S0269749116303116>

522 Cohen DD, Stelcer E, Santos FL, Prior M, Thompson C, Pabroa PCB. Fingerprinting and source  
523 apportionment of fine particle pollution in Manila by IBA and PMF techniques: A 7-year study. X-

524 Ray Spectrom [Internet]. 2009 Jan [cited 2013 Feb 14];38(1):18–25. Available from:  
525 <http://doi.wiley.com/10.1002/xrs.1112>

526 Diapouli E, Popovicheva O, Kistler M, Vratolis S, Persiantseva N, Timofeev M, et al. Physicochemical  
527 characterization of aged biomass burning aerosol after long-range transport to Greece from large  
528 scale wildfires in Russia and surrounding regions, Summer 2010. *Atmos Environ* [Internet]. Elsevier  
529 Ltd; 2014 Oct [cited 2014 Dec 2];96:393–404. Available from:  
530 <http://linkinghub.elsevier.com/retrieve/pii/S1352231014005858>

531 Dimitriou K, Remoundaki E, Mantas E, Kassomenos P. Spatial distribution of source areas of PM<sub>2.5</sub> by  
532 Concentration Weighted Trajectory (CWT) model applied in PM<sub>2.5</sub> concentration and composition  
533 data. *Atmos Environ* [Internet]. Elsevier Ltd; 2015;116:138–45. Available from:  
534 <http://www.sciencedirect.com/science/article/pii/S1352231015301631>

535 Eleftheriadis K, Balis D, Ziomas I, Colbeck I, Manalis N. Atmospheric aerosol and gaseous species in  
536 Athens, Greece. *Atmos Environ* [Internet]. 1998 Jun;32(12):2183–91. Available from:  
537 <http://linkinghub.elsevier.com/retrieve/pii/S1352231097004123>

538 Eleftheriadis K, Colbeck I. Coarse atmospheric aerosol: Size distributions of trace elements. *Atmos*  
539 *Environ*. 2001;35(31):5321–30.

540 Eleftheriadis K, Ochsenkuhn KM, Lympelopoulou T, Karanasiou A, Razos P, Ochsenkuhn-Petropoulou M.  
541 Influence of local and regional sources on the observed spatial and temporal variability of size  
542 resolved atmospheric aerosol mass concentrations and water-soluble species in the Athens  
543 metropolitan area. *Atmos Environ* [Internet]. Elsevier Ltd; 2014 Nov [cited 2014 Dec 18];97:252–  
544 61. Available from: <http://linkinghub.elsevier.com/retrieve/pii/S1352231014006074>

545 Endresen Ø, Sorgard E, Sundet JK, Dalsoren SB, Isaksen ISA, Berglen TF, et al. Emission from international  
546 sea transportation and environmental impact. *J Geophys Res* [Internet]. 2003 [cited 2015 Jan  
547 14];108(D17):4560. Available from: <http://doi.wiley.com/10.1029/2002JD002898>

548 Fridell E, Steen E, Peterson K. Primary particles in ship emissions. *Atmos Environ* [Internet]. 2008 Feb  
549 [cited 2014 Apr 24];42(6):1160–8. Available from:  
550 <http://linkinghub.elsevier.com/retrieve/pii/S1352231007009648>

551 Gerasopoulos E, Kouvarakis G, Babasakalis P, Vrekoussis M, Putaud J, Mihalopoulos N. Origin and  
552 variability of particulate matter (PM<sub>10</sub>) mass concentrations over the Eastern Mediterranean.  
553 *Atmos Environ* [Internet]. 2006 Aug [cited 2014 May 6];40(25):4679–90. Available from:  
554 <http://linkinghub.elsevier.com/retrieve/pii/S1352231006004043>

555 Grigoropoulos KN, Nastos PT, Ferentinos G. Spatial distribution of PM<sub>1</sub> and PM<sub>10</sub> during Saharan dust  
556 episodes in Athens, Greece. *Adv Sci Res*. 2009;3:59–62.

557 Hopke PK. A Review of Receptor Modeling Methods for Source Apportionment. *J Air Waste Manage*  
558 *Assoc* [Internet]. 2016;2247(January):10962247.2016.1140693. Available from:  
559 <http://www.tandfonline.com/doi/full/10.1080/10962247.2016.1140693>

560 Hopke PK, Ito K, Mar T, Christensen WF, Eatough DJ, Henry RC, et al. PM source apportionment and  
561 health effects : 1 . Intercomparison of source apportionment results. *J Expo Sci Environ Epidemiol*.  
562 2006;275–86.

563 Ito K, Christensen WF, Eatough DJ, Henry RC, Thurston GD. PM source apportionment and health  
564 effects : 2 . An investigation of intermethod variability in associations between source-apportioned  
565 fine particle mass and daily mortality in Washington, DC. *J Expo Sci Environ Epidemiol*.  
566 2006;2000:300–10.

567 Johnson KS, de Foy B, Zuberi B, Molina LT, Molina MJ, Xie Y, et al. Aerosol composition and source  
568 apportionment in the Mexico City Metropolitan Area with PIXE/PESA/STIM and multivariate  
569 analysis. *Atmos Chem Phys Discuss* [Internet]. 2006a May 19;6(3):3997–4022. Available from:  
570 <http://www.atmos-chem-phys-discuss.net/6/3997/2006/>

571 Johnson KS, de Foy B, Zuberi B, Molina LT, Molina MJ, Xie Y, et al. Aerosol composition and source  
572 apportionment in the Mexico City Metropolitan Area with PIXE/PESA/STIM and multivariate  
573 analysis. *Atmos Chem Phys Discuss* [Internet]. 2006b May 19;6(3):3997–4022. Available from:  
574 <http://www.atmos-chem-phys-discuss.net/6/3997/2006/>

575 Karanasiou A, Diapouli E, Cavalli F, Eleftheriadis K, Viana M, Alastuey A, et al. On the quantification of  
576 atmospheric carbonate carbon by thermal/optical analysis protocols. *Atmos Meas Tech*.  
577 2011;4(11):2409–19.

578 Karanasiou A, Mihalopoulos N. Air Quality in Urban Environments in the Eastern Mediterranean. In:  
579 Viana M, editor. *Handb Environ Chem* 26. Berlin: Springer; 2013. p. 219–38.

580 Karanasiou AA, Siskos PA, Eleftheriadis K. Assessment of source apportionment by Positive Matrix  
581 Factorization analysis on fine and coarse urban aerosol size fractions. *Atmos Environ* [Internet].  
582 Elsevier Ltd; 2009 Jul [cited 2013 Feb 13];43(21):3385–95. Available from:  
583 <http://linkinghub.elsevier.com/retrieve/pii/S1352231009002854>

584 Khillare PS, Sarkar S. Airborne inhalable metals in residential areas of Delhi, India: distribution, source  
585 apportionment and health risks. *Atmos Pollut Res* [Internet]. 2012 Jan 1 [cited 2014 Mar 10];3:46–  
586 54. Available from: <http://www.atmospollutres.com/articles/Volume3/issue1/APR-12-004.pdf>

587 Kim E, Hopke PK. Source Apportionment of Fine Particles in Washington, DC, Utilizing Temperature-  
588 Resolved Carbon Fractions. *J Air Waste Manage Assoc* [Internet]. 2004 Jul [cited 2014 Apr  
589 4];54(7):773–85. Available from:  
590 <http://www.tandfonline.com/doi/abs/10.1080/10473289.2004.10470948>

591 Kim E, Hopke PK. Source characterization of ambient fine particles at multiple sites in the Seattle area.  
592 *Atmos Environ* [Internet]. 2008 Aug [cited 2014 May 27];42(24):6047–56. Available from:  
593 <http://linkinghub.elsevier.com/retrieve/pii/S1352231008003087>

594 Kim E, Larson T V, Hopke PK, Slaughter C, Sheppard LE, Claiborn C. Source identification of PM<sub>2.5</sub> in an  
595 arid Northwest U.S. City by positive matrix factorization. *Atmos Res* [Internet]. 2003 May [cited  
596 2013 Feb 20];66(4):291–305. Available from:  
597 <http://linkinghub.elsevier.com/retrieve/pii/S0169809503000255>

598 Kioumourtzoglou M-A a, Coull B a, Dominici F, Koutrakis P, Schwartz J, Suh H. The impact of source  
599 contribution uncertainty on the effects of source-specific PM<sub>2.5</sub> on hospital admissions: a case  
600 study in Boston, MA. *J Expo Sci Environ Epidemiol* [Internet]. Nature Publishing Group;  
601 2014;24(4):365–71. Available from:  
602 [http://www.pubmedcentral.nih.gov/articlerender.fcgi?artid=4063325&tool=pmcentrez&rendertype=](http://www.pubmedcentral.nih.gov/articlerender.fcgi?artid=4063325&tool=pmcentrez&rendertype=abstract)  
603 <http://dx.doi.org/10.1038/jes.2014.7>

604 Kostenidou E, Florou K, Kaltsonoudis C, Tsiflikiotou M, Vratolis S, Eleftheriadis K, et al. Sources and  
605 chemical characterization of organic aerosol during the summer in the eastern Mediterranean.  
606 *Atmos Chem Phys*. 2015;15(19):11355–71.

607 Kostenidou E, Kaltsonoudis C, Tsiflikiotou M, Louvaris E, Russell LM, Pandis SN. Burning of olive tree  
608 branches: a major organic aerosol source in the Mediterranean. *Atmos Chem Phys Discuss*  
609 [Internet]. 2013 Mar 19 [cited 2013 Mar 20];13(3):7223–66. Available from: <http://www.atmos-chem-phys-discuss.net/13/7223/2013/>

611 Lazaridis M, Eleftheriadis K, Smolik J, Colbeck I, Kallos G, Drossinos Y, et al. Dynamics of fine particles and  
612 photo-oxidants in the Eastern Mediterranean (SUB-AERO). *Atmos Environ* [Internet]. 2006 Oct  
613 [cited 2014 Dec 18];40:6214–28. Available from:  
614 <http://linkinghub.elsevier.com/retrieve/pii/S1352231005005029>

615 Lee JH, Yoshida Y, Turpin BJ, Hopke PK, Poirot RL, Liou PJ, et al. Identification of Sources Contributing to  
616 Mid-Atlantic Regional Aerosol. *J Air Waste Manage Assoc* [Internet]. 2002 Oct [cited 2014 Apr  
617 4];52(10):1186–205. Available from:  
618 <http://www.tandfonline.com/doi/abs/10.1080/10473289.2002.10470850>

619 Li Z, Hopke PK, Husain L, Qureshi S, Dutkiewicz V a., Schwab JJ, et al. Sources of fine particle composition  
620 in New York city. *Atmos Environ* [Internet]. 2004 Dec [cited 2013 Feb 7];38(38):6521–9. Available  
621 from: <http://linkinghub.elsevier.com/retrieve/pii/S1352231004008192>

622 Liang CS, Duan FK, He K Bin, Ma YL. Review on recent progress in observations, source identifications  
623 and countermeasures of PM<sub>2.5</sub>. *Environ Int* [Internet]. Elsevier Ltd; 2016;86:150–70. Available  
624 from: <http://dx.doi.org/10.1016/j.envint.2015.10.016>

625 Liao H-T, Chou CC-K, Chow JC, Watson JG, Hopke PK, Wu C-F. Source and risk apportionment of selected  
626 VOCs and PM<sub>2.5</sub> species using partially constrained receptor models with multiple time resolution  
627 data. *Environ Pollut* [Internet]. Elsevier Ltd; 2015;205:121–30. Available from:  
628 <http://www.sciencedirect.com/science/article/pii/S0269749115002699>

629 Manousakas M, Diapouli E, Papaefthymiou H, Migliori a., Karydas a. G, Padilla-Alvarez R, et al. Source  
630 apportionment by PMF on elemental concentrations obtained by PIXE analysis of PM<sub>10</sub> samples  
631 collected at the vicinity of lignite power plants and mines in Megalopolis, Greece. *Nucl Instruments*  
632 *Methods Phys Res Sect B Beam Interact with Mater Atoms* [Internet]. Elsevier B.V.; 2015;349:114–  
633 24. Available from: <http://linkinghub.elsevier.com/retrieve/pii/S0168583X15001548>

634 Manousakas M, Eleftheriadis K, Papaefthymiou H. Characterization of PM<sub>10</sub> Sources and Ambient Air  
635 Concentration Levels at Megalopolis City (Southern Greece) Located in the Vicinity of Lignite-Fired  
636 Plants. *Aerosol Air Qual Res* [Internet]. 2013 [cited 2013 Apr 19];13(3):804–17. Available from:  
637 [http://www.aaqr.org/Doi.php?id=2\\_AAQR-12-09-OA-0239&v=13&i=3&m=6&y=2013](http://www.aaqr.org/Doi.php?id=2_AAQR-12-09-OA-0239&v=13&i=3&m=6&y=2013)

638 Manousakas M, Papaefthymiou H, Eleftheriadis K, Katsanou K. Determination of water-soluble and  
639 insoluble elements in PM<sub>2.5</sub> by ICP-MS. *Sci Total Environ* [Internet]. Elsevier B.V.; 2014 Jun 30  
640 [cited 2014 Jul 9];493C:694–700. Available from: <http://www.ncbi.nlm.nih.gov/pubmed/24992462>

641 Mantas E, Remoundaki E, Halari I, Kassomenos P, Theodosi C, Hatzikioseyan A, et al. Mass closure and  
642 source apportionment of PM<sub>2.5</sub> by Positive Matrix Factorization analysis in urban Mediterranean  
643 environment. *Atmos Environ* [Internet]. Elsevier Ltd; 2014;94:154–63. Available from:  
644 <http://dx.doi.org/10.1016/j.atmosenv.2014.05.002>

645 Marcazzan GM, Ceriani M, Valli G, Vecchi R. Source apportionment of PM<sub>10</sub> and PM<sub>2.5</sub> in Milan (Italy)  
646 using receptor modelling. *Sci Total Environ* [Internet]. 2003 Dec 30 [cited 2014 Mar 14];317(1-  
647 3):137–47. Available from: <http://www.ncbi.nlm.nih.gov/pubmed/14630417>

648 Moon KJ, Han JS, Ghim YS, Kim YJ. Source apportionment of fine carbonaceous particles by positive  
649 matrix factorization at Gosan background site in East Asia. *Environ Int*. 2008;34(5):654–64.

650 Niemi J V., Tervahattu H, Vehkamäki H, Kulmala M, Koskentalo T, Sillanpää M, et al. Characterization and  
651 source identification of a fine particle episode in Finland. *Atmos Environ*. 2004;38:5003–12.

652 Norris G, Brown S. EPA Positive Matrix Factorization (PMF) 5.0 Fundamentals and User Guide. EPA PMF  
653 5.0 Man. 2014;

654 Ostro B, Tobias A, Karanasiou A, Samoli E, Querol X, Rodopoulou S, et al. The risks of acute exposure to  
655 black carbon in Southern Europe: results from the MED-PARTICLES project. *Occup Environ Med*  
656 [Internet]. 2014 Nov 10 [cited 2014 Dec 13];1–7. Available from:  
657 <http://www.ncbi.nlm.nih.gov/pubmed/25385880>

658 Paatero P. The Multilinear Engine—A Table-Driven, Least Squares Program for Solving Multilinear  
659 Problems, Including the n -Way Parallel Factor Analysis Model. *J Comput Graph Stat* [Internet].  
660 1999;8(October 2014):854–88. Available from:  
661 <http://dx.doi.org/10.1080/10618600.1999.10474853>

662 Paatero P, Eberly S, Brown SG, Norris G a. Methods for estimating uncertainty in factor analytic  
663 solutions. *Atmos Meas Tech* [Internet]. 2014 Mar 27 [cited 2014 Jun 12];7(3):781–97. Available  
664 from: <http://www.atmos-meas-tech.net/7/781/2014/>

665 Paatero P, Hopke PK. Rotational tools for factor analytic models. *J Chemom* [Internet]. 2008 Feb [cited  
666 2014 Jun 15];23(2):91–100. Available from: <http://doi.wiley.com/10.1002/cem.1197>

667 Paatero P, Hopke PK, Song X-H, Ramadan Z. Understanding and controlling rotations in factor analytic  
668 models. *Chemom Intell Lab Syst* [Internet]. 2002 Jan;60(1-2):253–64. Available from:  
669 <http://linkinghub.elsevier.com/retrieve/pii/S0169743901002003>

670 Paatero P, Tappert U. Positive Matrix Factorization : A non-negative factor model with optimal utilization  
671 of error estimates of data values. *Environmetrics*. 1994;5:111–26.

672 Pandolfi M, Gonzalez-Castanedo Y, Alastuey A, de la Rosa JD, Mantilla E, de la Campa a S, et al. Source  
673 apportionment of PM(10) and PM(2.5) at multiple sites in the strait of Gibraltar by PMF: impact of  
674 shipping emissions. *Environ Sci Pollut Res Int* [Internet]. 2011 Feb [cited 2014 Apr 24];18(2):260–9.  
675 Available from: <http://www.ncbi.nlm.nih.gov/pubmed/20623340>

676 Pateraki S, Assimakopoulos VD, Bougiatioti A, Kouvarakis G, Mihalopoulos N, Vasilakos C. Carbonaceous  
677 and ionic compositional patterns of fine particles over an urban Mediterranean area. *Sci Total*  
678 *Environ* [Internet]. Elsevier B.V.; 2012;424:251–63. Available from:  
679 <http://dx.doi.org/10.1016/j.scitotenv.2012.02.046>

680 Pikridas M, Tasoglou A, Florou K, Pandis SN. Characterization of the origin of fine particulate matter in a  
681 medium size urban area in the Mediterranean. *Atmos Environ* [Internet]. Elsevier Ltd; 2013 Dec  
682 [cited 2014 Jan 9];80:264–74. Available from:  
683 <http://linkinghub.elsevier.com/retrieve/pii/S1352231013006018>

684 Polissar V, Hopke PK, Paatero P, Malm WC, Sisler JF. Atmospheric aerosol over Alaska 2 . Elemental  
685 composition and sources. *J Geophys Res*. 1998;103:19045–57.

686 Querol X, Alastuey A, Puigercus JA, Mantilla E, Ruiz CR, Lopez-Soler A, et al. Seasonal Evolution of  
687 Suspended Particles Around a Large Coal-Fired Power Station: Chemical Characterization. *Atmos*  
688 *Environ*. 1998;32(4):719–31.

689 Querol X, Alastuey A, Rodriguez S, Plana F, Ruiz CR, Cots N, et al. PM10 and PM2 . 5 source  
690 apportionment in the Barcelona Metropolitan area , Catalonia , Spain. *Atmos Environ*.  
691 2001;35:6407–19.

692 Reff A, Eberly SI, Bhavsar P V. Receptor Modeling of Ambient Particulate Matter Data Using Positive  
693 Matrix Factorization: Review of Existing Methods. *J Air Waste Manage Assoc* [Internet]. 2007 Feb  
694 [cited 2013 Aug 1];57(2):146–54. Available from:  
695 <http://www.tandfonline.com/doi/abs/10.1080/10473289.2007.10465319>

696 Ricard V, Jaffrezo J. Two years of continuous aerosol measurements in northern Finland. *J Geophys Res*.

697 2002;107:ACH 10 1–17.

698 Saffari A, Daher N, Samara C, Voutsas D, Kouras A, Manoli E, et al. Increased biomass burning due to the  
699 economic crisis in Greece and its adverse impact on wintertime air quality in Thessaloniki. *Environ*  
700 *Sci Technol* [Internet]. 2013 Dec 3;47(23):13313–20. Available from:  
701 <http://www.ncbi.nlm.nih.gov/pubmed/24187932>

702 Saraga DE, Makrogkika A, Karavoltos S, Sakellari A, Diapouli E, Eleftheriadis K, et al. A Pilot Investigation  
703 of PM Indoor/Outdoor Mass Concentration and Chemical Analysis during a Period of Extensive  
704 Fireplace Use in Athens. *Aerosol Air Qual Res* [Internet]. 2015;15(7):2485–95. Available from:  
705 [http://www.aaqr.org/Doi.php?id=1\\_AAQR-15-02-SIUAHE-0100&v=15&i=7&m=12&y=2015](http://www.aaqr.org/Doi.php?id=1_AAQR-15-02-SIUAHE-0100&v=15&i=7&m=12&y=2015)

706 Schaap M, van Loon M, ten Brink HM, Dentener FJ, Builtjes PJH. Secondary inorganic aerosol simulations  
707 for Europe with special attention to nitrate. *Atmos Chem Phys* [Internet]. 2004 Jun 15;4(3):857–74.  
708 Available from: <http://www.atmos-chem-phys.net/4/857/2004/>

709 Squizzato S, Masiol M, Brunelli A, Pistollato S, Tarabotti E, Rampazzo G, et al. Factors determining the  
710 formation of secondary inorganic aerosol: a case study in the Po Valley (Italy). *Atmos Chem Phys*  
711 [Internet]. 2013 Feb 19 [cited 2014 Mar 21];13(4):1927–39. Available from: <http://www.atmos-chem-phys.net/13/1927/2013/>

713 Stockwell WR, Kuhns H, Etyemezian V, Green MC, Chow JC, Watson JG, et al. The Treasure Valley  
714 secondary aerosol study II: modeling of the formation of inorganic secondary aerosols and  
715 precursors for southwestern Idaho. *Atmos Environ* [Internet]. 2003 Feb [cited 2014 Apr  
716 23];37(4):525–34. Available from: <http://linkinghub.elsevier.com/retrieve/pii/S1352231002008956>

717 Viana M, Amato F, Alastuey A, Querol X, Moreno T, Dos Santos SG, et al. Chemical tracers of particulate  
718 emissions from commercial shipping. *Environ Sci Technol* [Internet]. 2009 Oct 1;43(19):7472–7.  
719 Available from: <http://www.ncbi.nlm.nih.gov/pubmed/19848163>

720 Viana M, Hammingh P, Colette A, Querol X, Degraeuwe B, Vlioger I De, et al. Impact of maritime  
721 transport emissions on coastal air quality in Europe. *Atmos Environ* [Internet]. Elsevier Ltd; 2014  
722 Jun [cited 2014 Jun 4];90:96–105. Available from:  
723 <http://linkinghub.elsevier.com/retrieve/pii/S1352231014002313>

724 Viana M, Kuhlbusch T a. J, Querol X, Alastuey A, Harrison RM, Hopke PK, et al. Source apportionment of  
725 particulate matter in Europe: A review of methods and results. *J Aerosol Sci* [Internet]. 2008 Oct  
726 [cited 2013 Jan 30];39(10):827–49. Available from:  
727 <http://linkinghub.elsevier.com/retrieve/pii/S0021850208001018>

728 Viana M, Reche C, Amato F, Alastuey a., Querol X, Moreno T, et al. Evidence of biomass burning  
729 aerosols in the Barcelona urban environment during winter time. *Atmos Environ* [Internet].  
730 Elsevier Ltd; 2013 Jun [cited 2014 Sep 9];72:81–8. Available from:  
731 <http://linkinghub.elsevier.com/retrieve/pii/S1352231013001325>

732 Waked a., Favez O, Alleman LY, Piot C, Petit JE, Delaunay T, et al. Source apportionment of PM10 in a  
733 north-western Europe regional urban background site (Lens, France) using positive matrix  
734 factorization and including primary biogenic emissions. *Atmos Chem Phys*. 2014;14(7):3325–46.

735 Yin J, Allen AG, Harrison RM, Jennings SG, Wright E, Fitzpatrick M, et al. Major component composition  
736 of urban PM10 and PM2.5 in Ireland. *Atmos Res* [Internet]. 2005 Dec [cited 2014 Feb 21];78(3-  
737 4):149–65. Available from: <http://linkinghub.elsevier.com/retrieve/pii/S0169809505001249>

738

739

740

741